Electrochemical Oxidation and Reduction of Flavin Mononucleotide Adsorbed on a Mercury Electrode Surface

Tadaaki KAKUTANI,* Kenji KANO, Shinji ANDO, and Mitsugi SENDA
Department of Agricultural Chemistry, Faculty of Agriculture, Kyoto University, Kyoto 606
(Received Augast 4, 1980)

The electrochemical redox reaction of flavin mononucleotide (FMN) adsorbed on a hanging mercury drop electrode was studied in a pH 6.9 phosphate buffer and a pH 4.9 acetate buffer by means of cyclic d.c. and phasese lective a.c. voltammetry. Both the oxidized and reduced forms of FMN are strongly adsorbed on the electrode surface, and a stable adsorption layer of FMN($(FMN)_{ad}$) is formed. The cyclic d.c. and a.c. voltammetric behavior of $(FMN)_{ad}$ is explained by equations for a two-step one-electron surface redox reaction. The formal standard redox potentials, semiquinone formation constants, and charge transfer-rate constants of the surface redox reaction of FMN at the mercury electrode were determined.

Recently an increasing number of papers have appeared regarding redox-modified electrodes, which are prepared by attaching redox species, by chemical binding or irreversible adsorption, to the surface of an electrode material (for reviews, see Refs. 1 and 2). Electrocatalysis and electroanalysis have been in particular considered as possible applications of these electrodes. In such applications, data are essential on the kinetics of the surface redox reaction, *i.e.*, the electrode processes exhibited by redox species confined to the electrode surface. In previous papers, we have presented theories of a.c. polarography and voltammetry for simple one-step[3] and two-step surface redox reactions.[4] The theories have also been applied to the electrode processes of ferredoxins irreversibly adsorbed on the mercury electrode surface.[5,6]

The electrochemical behavior of flavin mononucleotide(FMN) has been studied by many authors (for review, see Ref. 7). Senda *et al.*[8] have shown by a.c. polarography that both the oxidized and reduced forms of FMN are adsorbed on the mercury electrode surface; this was confirmed by Takemori[9] and by Hartley and Wilson.[10] However, these authors did not consider the surface redox reaction of FMN, which will be discussed below. In this work, the electrochemical redox reaction of FMN adsorbed on the surface of the hanging mercury drop electrode (HMDE) has been studied in terms of the surface redox reaction, using cyclic d.c. and a.c. voltammetric techniques. We have also determined the kinetic and thermodynamic parameters of the surface redox reaction of FMN. The results and discussion are presented here.

Experimental

Chemicals. Flavin mononucleotide(FMN), a reagent-grade chemical purchased from Nakarai Chemicals Co., was used without further purification. The supporting electrolyte salt and buffers were commercially available reagent-grade materials, used as received. Triply distilled water was used to prepare the electrolysis solution.

Electrochemical Measurements. Cyclic d.c. voltammograms were obtained with a potentiostat, Yanaco Model PE-21-TB2S, equipped with a function generator, YHP 3310B or Nikko Keisoku Model NFG-3. The a.c. voltammetric measurements were performed with a lock-in amplifier, NF LI-574, equipped with the above potentiostat system. A lock-in amplifier, NF LI-572B, was used as an a.c. signal generator. This instrumental system allows the simultaneous measurement of the real (in-phase) and imaginary(out-of-phase) components of the a.c. voltammetric current, which are recorded against the d.c. sweep voltage applied to a hanging mercury drop electrode (HMDE).

All the voltammetric measurements were made under potentiostatic conditions with a three-electrode system consisting of a hanging mercury drop working electrode, a coiled platinum wire auxiliary electrode, and a saturated calomel reference electrode(SCE). The HMDE was a Metrohm drop electrode E 410, the surface area of which was 0.0187 ± 0.0003 cm^2. Buffer solutions (0.2 mol dm^{-3} acetic acid–sodium acetate for pH 4.9 and 0.2 mol dm^{-3} sodium dihydrogenphosphate–disodium hydrogenphosphate for pH 6.9) were used as the base solutions. The ionic strength of a base solution was adjusted to 0.5 mol dm^{-3} with potassium nitrate. A fresh mercury drop from the HMDE was exposed to the electrolysis solution for a given period of time, to be referred to as the exposure time, t_{exp}, below, while the potential of the HMDE was controlled at a constant d.c. potential(E_i). Then the d.c. voltage scan was started from E_i, with scan rates of $v=0.091$ V s^{-1} for cyclic d.c. voltammetry and of $v=0.036$ V s^{-1} for a.c. voltammetry, unless otherwise stated. In a.c. voltammetry, the amplitude of the superimposed a.c. voltage was adjusted to 10 mV (peak to peak) throughout the frequency range of 100—500 Hz. To avoid possible photochemical decomposition of FMN, electrochemical measurements were performed in a dark box at 25 °C under a nitrogen atmosphere.

Results

In order to study the surface redox reaction of FMN, electrochemical measurements were performed at concentrations of FMN lower than 4×10^{-6} mol dm^{-3}, at which the current resulting from unadsorbed, diffusing FMN will be negligibly small.

Figure 1 shows a linear potential sweep voltammogram of 1.5×10^{-6} mol dm^{-3} FMN in a pH 6.9 phosphate buffer, which was recorded after $t_{exp}=2$ min at $E_i=+0.15$ V. At such a low concentration, FMN gave two peaked-shaped waves centered at +0.05 V and −0.41 V, but no ordinary diffusion wave was observed. According to Senda *et al.*[8] and Breyer and Biegler,[11] the reduction wave observed at +0.05 V may be due to the dissolution of the mercury electrode by FMN. Thus, in this study, the electrochemical behavior of the wave observed at −0.41 V was investigated in detail.

Cyclic D.c. Voltammetry. Figure 2A shows the cyclic voltammogram of 9×10^{-7} mol dm^{-3} FMN at

Table 1. Scan-rate dependence of the peak current, peak potential, and half-peak width of cyclic d.c. voltammograms of FMN adsorbed on a mercury electrode at pH 6.9[a]

Scan rate/mV s^{-1}	I_{pc}/μA	I_{pa}/μA	E_{pc}^{DC}/V[b]	E_{pa}^{DC}/V[b]	$\Delta E_{p/2,c}^{DC}$/mV	$\Delta E_{p/2,a}^{DC}$/mV
34	0.068	0.073	−0.41	−0.41	68	68
47	0.100	0.104	−0.41	−0.41	68	68
91	0.180	0.181	−0.41	−0.41	68	68
181	0.335	0.336	−0.41	−0.41	70	69

a) $C_{FMN}=9\times10^{-7}$ mol dm^{-3}, $t_{exp}=3$ min at $E_i=-0.20$ V *vs.* SCE. b) V *vs.* SCE.

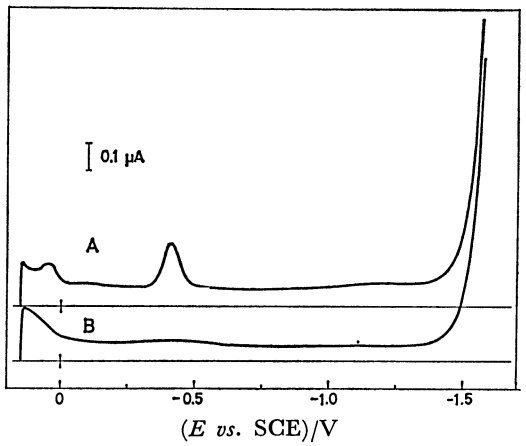

Fig. 1. Linear potential sweep voltammograms recorded after $t_{exp}=2$ min at $E_i=+0.15$ V *vs.* SCE in pH 6.9 phosphate buffer containing (A) 1.5×10^{-6} mol dm^{-3} FMN and (B) no FMN.

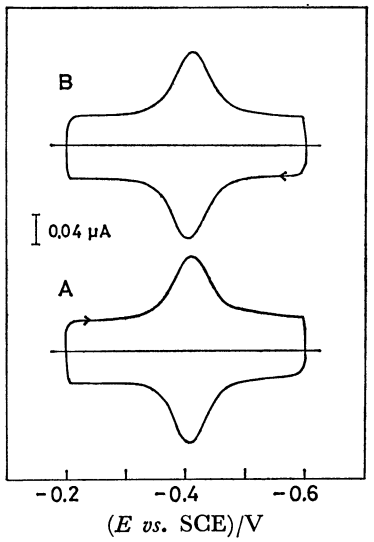

Fig. 2. Cyclic d.c. voltammograms of 9×10^{-7} mol dm^{-3} FMN in pH 6.9 phosphate buffer. Voltage scan was started after $t_{exp}=1$ min from (A) $E_i=-0.2$ V *vs.* SCE and (B) $E_i=-0.6$ V *vs.* SCE.

pH 6.9, which was recorded after $t_{exp}=1$ min at $E_i=-0.2$ V with the HMDE. A pair of cathodic and anodic waves was observed at −0.41 V. The shapes and heights of these two waves were practically identical expect for the opposite current sign. The waves grew to a certain limit, the maximum peak height I_{pc}^{max} or I_{pa}^{max}, with an increase in the concentration of FMN at a constant exposure time or with

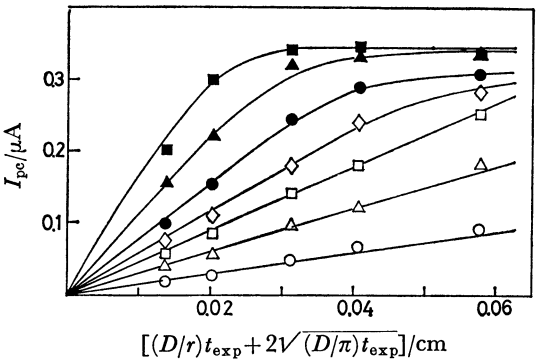

Fig. 3. Plot of I_{pc} against $[(D/r)t_{exp}+2(D/\pi)^{1/2}t_{exp}^{1/2}]$ in pH 6.9 phosphate buffer. FMN concentrations are: (○) 3×10^{-7} mol dm^{-3}; (△) 6×10^{-7} mol dm^{-3}; (□) 9×10^{-7} mol dm^{-3}; (◇) 1.2×10^{-6} mol dm^{-3}; (●) 1.8×10^{-6} mol dm^{-3}; (▲) 3×10^{-6} mol dm^{-3}; (■) 4×10^{-6} mol dm^{-3}.

an increase in the exposure time at a constant concentration of FMN, indicating that the waves are due to the FMN accumulated on the HMDE surface. The t_{exp} dependence of the cathodic peak height, I_{pc}, obtained with $E_i=-0.2$ V is shown in Fig. 3 for different FMN concentrations at pH 6.9. At lower concentrations, I_{pc} was proportional to the $[(D/r)t_{exp}+2(D/\pi)^{1/2}t_{exp}^{1/2}]$ function, where D is the diffusion coefficient of FMN, which was estimated by means of the Ilkovič equation to be 3.2×10^{-6} cm^2 s^{-1} in the pH range of 4.9—6.9, and where r is the radius of the HMDE, which was determined to be 0.038 cm. The slope of the plot was also proportional to the concentration of FMN. These results indicate the diffusion-controlled adsorption of FMN at the electrode surface.[5,13] A similar dependence of the peak height on t_{exp} was observed also for the anodic wave. However, the maximum value of the anodic peak height, I_{pa}^{max}, was slightly larger than that of the cathodic peak height, I_{pc}^{max}; *i.e.*, $I_{pa}^{max}/I_{pc}^{max}\simeq1.1$ (see Fig. 5A).

Table 1 summarizes the peak heights, I_{pc} and I_{pa}; the peak potentials, E_{pc}^{DC} and E_{pa}^{DC}, and the half-peak widths, $\Delta E_{p/2,c}^{DC}$ and $\Delta E_{p/2,a}^{DC}$, of the cathodic and anodic waves respectively, which were recorded with various scan rates after $t_{exp}=3$ min at $E_i=-0.2$ V in a pH 6.9 phosphate buffer containing 9×10^{-7} mol dm^{-3} of FMN. Both I_{pc} and I_{pa} were proportional to the voltage scan rate, v. The I_{pa}/I_{pc} ratio was unity when corrected for the difference between the amounts of the adsorbed FMN at E_{pc}^{DC} and E_{pa}^{DC} due to the different t_{exp} values. E_{pc}^{DC} and E_{pa}^{DC} coincided with each other and are independent

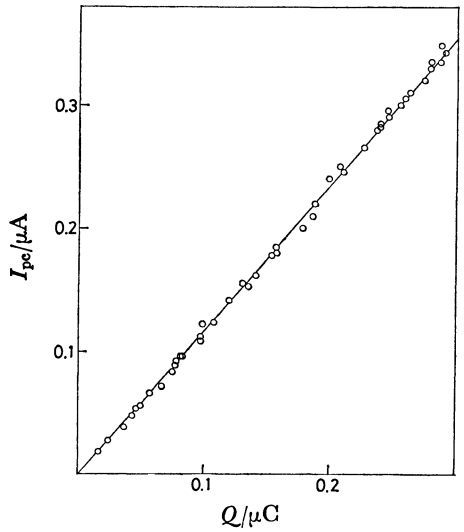

Fig. 4. Plot of I_{pc} against Q at pH 6.9.

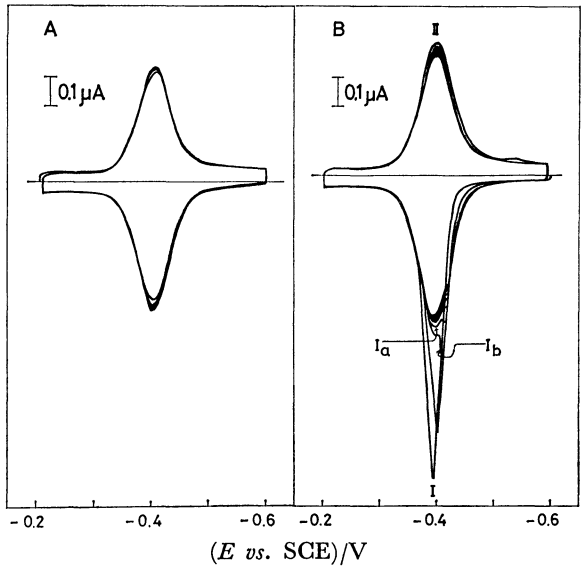

Fig. 5. Cyclic d.c. voltammograms of 4×10^{-6} mol dm^{-3} FMN in pH 6.9 phosphate buffer. Voltage scan was started after $t_{exp}=3$ min from (A) $E_i=-0.2$ V *vs.* SCE and (B) $E_i=-0.6$ V *vs.* SCE.

of the v. The half-peak widths were 68 mV over the scan rate range of 34 mV s^{-1} to 181 mV s^{-1}. The peak height of either wave was proportional to the electricity, Q, required to reduce or oxidize the FMN adsorbed on the electrode surface, which was estimated from the area under the wave, as is shown in Fig. 4. This indicates that the peak height is directly proportional to the amount of the FMN adsorbed on the electrode surface until the peak height reaches a maximum value. On the other hand, the peak potentials and half-peak widths were practically independent of the amount of the adsorbed FMN. These results indicate that the reaction corresponding to the waves is a reversible surface redox reaction.[4]

When the electrode was exposed to the FMN solution at potentials much more negative than the redox potential of the adsorbed FMN, *e.g.*, −0.6 V at pH

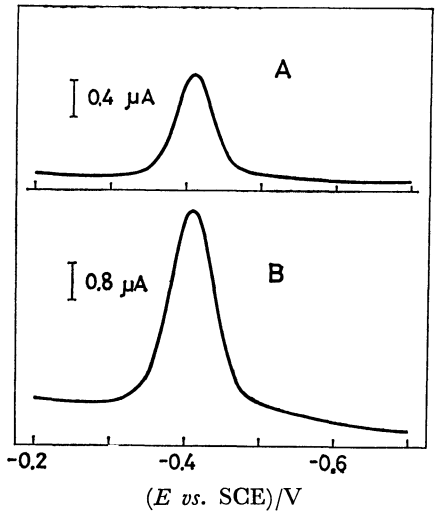

Fig. 6. A.c. voltammograms of 3×10^{-7} mol dm^{-3} FMN in pH 6.9 phosphate buffer at 300 Hz. D.c. voltage scan was started from $E_i=-0.2$ V *vs.* SCE after $t_{exp}=5$ min. (A): Real component, (B): imaginary component.

6.9, the adsorbed FMN was reduced to form an adsorbed layer of leuco-FMN on the electrode surface. The cyclic voltammetric behavior of this adsorbed leuco-FMN was the same as that of adsorbed FMN, provided that the surface coverage was low, as is shown in Fig. 2. However, as the surface coverage increased, the cyclic voltammograms observed were remarkably different in shape and height from that of the adsorbed FMN. Figure 5 shows the cyclic voltammograms of FMN at pH 6.9, which were recorded after the electrode had been exposed to a solution containing 4×10^{-6} mol dm^{-3} of FMN for $t_{exp}=3$ min at $E_i=-0.2$ V (Fig. 5A) and at $E_i=-0.6$ V (Fig. 5B). When FMN was adsorbed at $E_i=-0.2$ V, a symmetrical voltammogram was obtained as has been stated above; in succeeding cycles of the voltage scan between −0.2 V and −0.6 V, the peak heights and shapes of the cathodic and anodic waves remained practically unchanged (Fig. 5A). On the contrary, when FMN was adsorbed at $E_i=-0.6$ V, in the first voltage scan from −0.6 V to −0.2 V an asymmetric anodic wave was observed at −0.39 V (Wave I); its peak height was about three times that of the anodic wave in Fig. 5A. Upon the reversal of the voltage scan at −0.2 V, a symmetrical cathodic wave (Wave II) was observed at −0.40 V; its peak height was slightly larger than that of the cathodic wave in Fig. 5A. In the successive cycles of the voltage scan, Wave I decreased in height and split into two peaks, I_a and I_b, while Waves I_a, I_b, and II decreased in height until a steady state was attained. The steady-state cyclic voltammograms were nearly symmetric, and their peak heights were, though dependent on the bulk concentration of FMN, slightly higher than that of the wave in Fig. 5A, *i.e.*, the maximum peak height of the voltammogram produced by FMN adsorbed at $E_i=-0.2$ V. Similar behavior was observed also in the pH 4.9 acetate buffer.

A.c. Voltammetry. In the cyclic a.c. voltammetry

Table 2. Peak potential and half-peak width of a.c. voltammograms of FMN adsorbed on a mercury electrode at pH 6.9[a]

Frequency/Hz	E_p^{real}/V[b]	E_p^{imag}/V[b]	$\Delta E_{p/2}^{real}$/mV		$\Delta E_{p/2}^{imag}$/mV	
			Obsd	Calcd[c]	Obsd	Calcd[c]
100	−0.41	−0.41	53	52.4	68	67.0
200	−0.41	−0.41	54	53.1	69	68.3
300	−0.41	−0.41	55	54.2	71	70.4
400	−0.41	−0.41	56	55.6	73	73.3
500	−0.41	−0.41	59	57.3	78	76.7

a) $C_{FMN}=9\times10^{-7}$ mol dm^{-3}, $t_{exp}=2$ min at $E_i=-0.20$ V *vs.* SCE. b) V *vs.* SCE. c) Calculated by using $K=1.1$, $k_{sap}=4.9\times10^3$ s^{-1}, and $\theta_t=0.40$.

of FMN adsorbed at $E_i=-0.2$ V, the a.c. voltammogram of the cathodic scan was practically identical in height and shape with that of the anodic scan. Accordingly, the a.c. voltammetric behavior was studied only for the cathodic scan. Figure 6 shows a.c. voltammograms for FMN adsorbed on the HMDE at pH 6.9; the voltammograms were recorded after the electrode had been exposed to a solution containing 3×10^{-7} mol dm^{-3} FMN at $E_i=-0.2$ V for $t_{exp}=5$ min. In all the a.c. voltammograms recorded in this study, the peak potentials of the real and imaginary components, E_p^{real} and E_p^{imag}, were independent of the a.c. frequency between 100 and 500 Hz and independent of the amount of the adsorbed FMN; they coincided with each other and with the peak potentials of the corresponding cyclic d.c. waves, as is shown in Table 2. On the other hand, the peak currents, $\delta_1 I_p^{real}$ and $\delta_1 I_p^{imag}$, and the half-peak widths, $\Delta E_{p/2}^{real}$ and $\Delta E_{p/2}^{imag}$, of the real and imaginary components depended on the a.c. frequency and also on the amount of the adsorbed FMN, as may be seen in Fig. 8 and Table 2.

Discussion

Adsorption of FMN on the Mercury Electrode Surface. The present study has revealed that both the oxidized and reduced forms of FMN are strongly adsorbed on the HMDE surface; this finding is consistent with those of previous works.[8–10] The d.c. voltammetric data indicate that the adsorption of FMN is controlled by diffusion; at lower FMN concentrations, the peak height of the cyclic d.c. voltammogram is given by $I_p=kA\Gamma=kA[(D/r)t_{exp}+2(D/\pi)^{1/2}t_{exp}^{1/2}]C_{FMN}$, where k is the proportionality constant; A, the surface area of the HMDE; Γ, the surface concentration of FMN per unit of area; and C_{FMN}, the concentration of FMN in a bulk solution. At high concentrations, when the maximum current is attained, it is given by $I_p^{max}=kA\Gamma^{max}$, where Γ^{max} is the maximum value of Γ. By applying these two equations to such plots as are shown in Fig. 3, we estimated the maximum surface concentration of FMN adsorbed at −0.2 V, Γ_O^{max}, as $(6.7\pm0.1)\times10^{-11}$ mol cm^{-2} at pH 6.9 and $(9.5\pm0.4)\times10^{-11}$ mol cm^{-2} at pH 4.9. The Γ or Γ^{max} value can also be estimated from the area under the d.c. voltammetric wave, provided that m_1/n_1 and m_2/n_2 are assumed as unity;[3,4] $Q=nFA\Gamma$ and $Q_{max}=nFA\Gamma^{max}$, where n is the number of electrons transferred per molecule of FMN. For the cathodic wave this gave $\Gamma_O^{max}=(8.0\pm0.2)\times10^{-11}$ mole cm^{-2} at pH 6.9 and $(8.8\pm0.2)\times10^{-11}$ mol cm^{-2} at pH 4.9, by assuming $n=2$. The Γ_O^{max} values estimated by these two methods agree well with each other at either pH. When we assume that FMN is adsorbed on the electrode surface with its alloxazine-ring plane oriented parallel to the electrode surface, a CPK molecular model[14] gives $\Gamma_O^{max}=7.5\times10^{-11}$ mol cm^{-2}. On the other hand, when FMN was adsorbed at $E_i=-0.6$ V, the area under the anodic wave obtained with the first voltage scan increased with an increase in C_{FMN} and/or t_{exp} and did not attain a maximum value even at $C_{FMN}=4\times10^{-6}$ mol dm^{-3} and $t_{exp}=5$ min, at which the Γ_R estimated by $Q=nFA\Gamma$ was already larger than Γ_O^{max}. Accordingly, the maximum surface concentration of leuco-FMN, Γ_R^{max}, should be larger than Γ_O^{max}, but it could not be accurately estimated from the present d.c. voltammetric data.

The cyclic d.c. voltammetric behavior of FMN and leuco-FMN at high surface concentrations, shown in Fig. 5, should be interpreted as follows. Since $\Gamma_O^{max}<\Gamma_R^{max}$, the reduction of a complete monolayer of FMN would be followed by the further adsorption of FMN at potentials more negative than the redox potential of the adsorbed FMN, resulting in a higher surface concentration of leuco-FMN than the initial Γ_O^{max}. This would be explain why the anodic peak height is slightly larger than the preceding cathodic one for a complete monolayer of adsorbed FMN (see Fig. 5A). When the initial surface concentration of leuco-FMN, Γ_R, is larger than Γ_O^{max}, the oxidation of the monolayer of leuco-FMN should cause an immediate desorption of a part of the adsorbed FMN molecules. The distortion of the anodic wave (Wave I) and the appearance of Wave I_b, shown in Fig. 5B, may reflect the desorption process associated with the oxidation of the adsorbed leuco-FMN. Cyclic voltammograms of the repeated scans, illustrated in Fig. 5B, suggest that the desorption and adsorption processes are slow.

Surface Redox Reaction of FMN Adsorbed on HMDE. The cyclic d.c. and a.c. voltammetry behavior of FMN adsorbed on the electrode surface should be interpreted in terms of a two-step surface redox reaction:[7–10,12]

$$\begin{aligned} O_{ad} + n_1 e &\rightleftharpoons S_{ad} \\ S_{ad} + n_2 e &\rightleftharpoons R_{ad}. \end{aligned} \qquad (I)$$

When these two steps are d.c. reversible, the simplified equations (Case (I) in Ref. 4) of the cyclic d.c. voltammogram, I^{DC}, and the real and imaginary components of the a.c. current, $\delta_1 I_{corr}^{imag}$ and $\delta_1 I_{obsd}^{real}$, can be written, for $n_1=n_2=m_1=m_2=1$, as:

$$I^{DC} = I_F^{rev} = (F^2/RT)Av\Gamma_t \frac{[\rho^2(\sqrt{K}\rho+2)+\rho(\sqrt{K}+2\rho)]}{(1+\sqrt{K}\rho+\rho^2)^2}, \tag{1}$$

$$\delta_1 I_{obsd}^{real} = \delta_1 I_F^{real} = (F^2/RT)A\omega\Gamma_t\delta_1 E \frac{\sqrt{K}\rho\rho^{1/2}}{(1+\sqrt{K}\rho+\rho^2)} \times \frac{\lambda(\sqrt{K})^{1/2}(1+\rho)\{\sqrt{K}[\lambda^2\rho-(1+\sqrt{K}\rho+\rho^2)]+(\sqrt{K}+4\rho+\sqrt{K}\rho^2)(1+\sqrt{K})\}}{\{K[\lambda^2\rho-(1+\sqrt{K}\rho+\rho^2)]^2+\lambda^2(\sqrt{K})(1+\sqrt{K})^2(1+\rho)^2\rho\}}, \tag{2}$$

$$\delta_1 I_{corr}^{imag} = \delta_1 I_F^{imag} = (F^2/RT)A\omega\Gamma_t\delta_1 E \frac{\sqrt{K}\rho}{(1+\sqrt{K}\rho+\rho^2)} \times \frac{\{\rho\lambda^2(\sqrt{K})(1+\sqrt{K})(1+\rho)^2-\sqrt{K}[\lambda^2\rho-(1+\sqrt{K}\rho+\rho^2)](\sqrt{K}+4\rho+\sqrt{K}\rho^2)\}}{\{K[\lambda^2\rho-(1+\sqrt{K}\rho+\rho^2)]^2+\lambda^2(\sqrt{K})(1+\sqrt{K})^2(1+\rho)^2\rho\}}, \tag{3}$$

with:

$$K = \exp[(F/RT)(E'_{o1}-E'_{o2})]$$
$$\rho = \exp[(F/RT)(E-E'_o)]$$
$$E'_o = (E'_{o1}+E'_{o2})/2$$
$$\lambda = \omega/k_{sap}.$$

Here, it is further assumed that $\alpha_1=\alpha_2=\beta_1=\beta_2=0.5$ and $k_{sap}(1)=k_{sap}(2)=k_{sap}$, where α_i, β_i, and $k_{sap}(i)$ are the cathodic and anodic transfer coefficients and the apparent rate constant of the i-th charge transfer step respectively. In these equations, Γ_t is the total surface concentration per unit of area defined by $\Gamma_t=\Gamma_O+\Gamma_S+\Gamma_R$; E'_{o1} and E'_{o2} are the formal standard potentials of the first and second redox steps respectively, and ω and $\delta_1 E$ are the angular frequency and amplitude of the superimposed a.c. voltage respectively. E'_o corresponds to the formal standard potential of the adsorbed redox couple, O_{ad}/R_{ad}. The parameter K corresponds to the formation constant of the adsorbed semiquinone form, S_{ad}. The apparent rate constant, k_{sap}, depends on the adsorption parameters and on the total surface coverage, $\theta_t(\equiv\Gamma_t/\Gamma^{max})$; *i.e.*,

$$k_{sap} = k_{sap}(\theta_t\to 0)\exp(-a\theta_t), \tag{4}$$

where $k_{sap}(\theta_t\to 0)$ is the apparent rate constant at $\theta_t=0$.

When K is less than 16, Eq. 1 predicts that the cathodic and anodic d.c. voltammograms will have a maximum at E'_o, independently of v and Γ_t, *i.e.*, $E_{pc}^{DC}=E_{pa}^{DC}=E'_o$, and that the half-peak widths, $\Delta E_{p/2,c}^{DC}$ and $\Delta E_{p/2,a}^{DC}$, will have the same value, which is independent of v and Γ_t and which depends only on the K parameter:

$$\Delta E_{p/2,c}^{DC} = \Delta E_{p/2,a}^{DC} = (2RT/F)|\ln\xi|, \tag{5}$$

where ξ is the solution of the equation: $\xi^4-K\xi^3+(K-\sqrt{K}-6)\xi^2-K\xi+1=0$, and that the cathodic and anodic peak heights will be proportional to v and Γ_t:

$$I_{pc} = I_{pa} = 2(F^2/RT)A\Gamma_t v(2+\sqrt{K})^{-1} = (F/RT)vQ(2+\sqrt{K})^{-1}. \tag{6}$$

All the experimental results obtained in this work agreed well with these theoretical predictions (see Table 1 and Fig. 4). Thus, we determined the semiquinone formation constant, K, from the half-peak widths (Eq. 5) and from the slope of the I_p *vs.* Q plot (Eq. 6). The results are summarized in Table 3. The K values estimated by these two methods agreed well with each other at either pH.

Table 3. Semiquinone formation constants of FMN adsorbed on a mercury electrode at pH 6.9 and 4.9

pH	K	Method
6.9	1.2	$\Delta E_{p/2}^{DC}$
	1.0	I_{pc} *vs.* Q plot
4.9	0.82	$\Delta E_{p/2}^{DC}$
	0.62	I_{pc} *vs.* Q plot

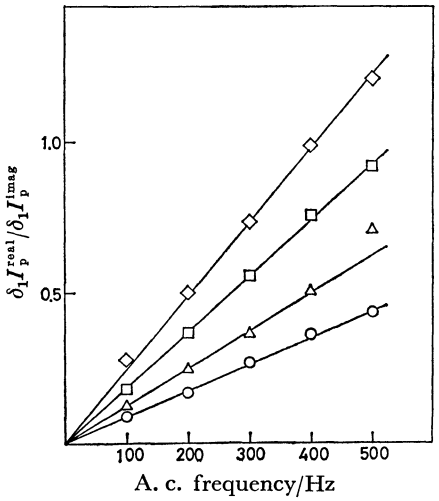

Fig. 7. Frequency dependence of the ratio of a.c. peak current, $(\delta_1 I_p^{real}/\delta_1 I_p^{imag})$, at various total surface coverages of FMN, θ_t, in pH 6.9 phosphate buffer. θ_t: (○) 0.24; (△) 0.40; (□) 0.84; (◇) 1.0.

According to Eqs. 2 and 3, the peak potentials of a.c. voltammograms, E_p^{real} and E_p^{imag}, should be independent of the a.c. frequency and should coincide with each other and with E'_o within a certain limited range of values of K and λ. Table 2 shows that the experimental results agree well with this prediction. In addition, the ratio of $\delta_1 I_F^{real}$ to $\delta_1 I_F^{imag}$ at $E=E'_o$ is given by:

$$(\delta_1 I_F^{real}/\delta_1 I_F^{imag})_{E=E'_o} = \omega/k_{sap}(K)^{1/4}. \tag{7}$$

Such a linear dependence of the current ratio on the a.c. frequency was proved for various total surface coverages, as is shown in Fig. 7, where θ_t was cal-

culated from the peak height of the corresponding cathodic d.c. voltammogram, *i.e.*, $\theta_t=(I_{pc}/I_{pc}^{max})$. The slope of this plot allows us to estimate the apparent rate constant, k_{sap}, provided that K is known. Table 4 summarizes the k_{sap} values estimated from such plots at various surface coverages using K values determined by d.c. voltammetry, *i.e.*, $K=1.1$ at pH 6.9 and $K=0.72$ at pH 4.9. Table 2 gives the experimental values of $\Delta E_{p/2}^{real}$ and $\Delta E_{p/2}^{imag}$ and the theoretical values calculated by using these values of K and k_{sap} at $\theta_t=0.4$. The a.c. peak currents are plotted against the a.c. frequency in Fig. 8, in which the solid lines are drawn by the use of Eqs. 2 and 3. The agreement between the experimental results and theoretical predictions is good. A good agreement between theory and experimental results was also obtained at other θ_t's. As may be seen from Eq. 4, a plot of ln k_{sap} against θ_t should yield a straight line with a slope of $-a$; this was experimentally verified, as is shown in Fig. 9. In conclusion, we can state that the cyclic d.c. and a.c. voltammetric behavior of the adsorbed FMN can be explained by the two-step surface redox mechanism (I). From E'_o and K, we can estimate the formal standard redox potentials of the first and second redox steps, E'_{o1} and E'_{o2}. Table 5 summarizes the values of $k_{sap}(\theta_t\rightarrow\theta)$ and a as well as the K, E'_o, E'_{o1} and E'_{o2} values determined above. For comparison, the standard redox potentials, E'_o(bulk), E'_{o1}(bulk), and E'_{o2}(bulk), and the semiquinone formation constant, K(bulk), for the redox reaction of FMN in a bulk solution[12] are given in Table 5. A comparison of the formal standard potentials of the surface redox reaction with those of the redox reaction in a bulk solution gives $\Delta E_1=E'_{o1}-E'_{o1}$(bulk)$\simeq+70$ mV and $\Delta E_2=E'_{o2}-E'_{o2}$(bulk)$\simeq+10$ mV at pH 6.9 and $\Delta E_1\simeq+60$ mV and $\Delta E_2\simeq0$ at pH 4.9. These results suggest that[4] the increasing adsorbability of FMN on the mercury electrode surface is in the order of the oxidized form<the semiquinone form$\simeq$the reduced form; this order is consistent with the findings of previous works.[7-10]

Table 4. The apparent rate constants of the surface redox reaction of FMN adsorbed on a mercury electrode at pH 6.9 and 4.9

pH 6.9		pH 4.9	
θ_t	$k_{sap}/10^3$ s^{-1}	θ_t	$k_{sap}/10^3$ s^{-1}
0.17	7.9	0.20	7.9
0.25	7.1	0.25	7.7
0.40	4.9	0.33	6.5
0.75	3.4	0.49	4.9
0.84	3.3	0.59	4.6
0.88	3.2	0.79	3.8
1.0	2.4	0.89	3.5

This work was supported by a Grant-in-Aid for Scientific Research No. 411706 from the Japanese Ministry of Education, Science and Culture.

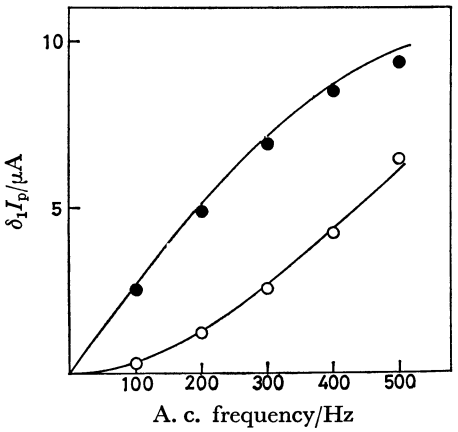

Fig. 8. Dependence of the a.c. peak currents of 9×10^{-7} mol dm^{-3} FMN on a.c. frequency at pH 6.9. A.c. voltammograms were recorded after $t_{exp}=2$ min at $E_1=-0.2$ V *vs.* SCE. ○: Real component, ●: imaginary component. Solid lines: theoretical curves ($K=1.1$, $k_{sap}=4.9\times10^3$ s^{-1} and $\theta_t=0.40$).

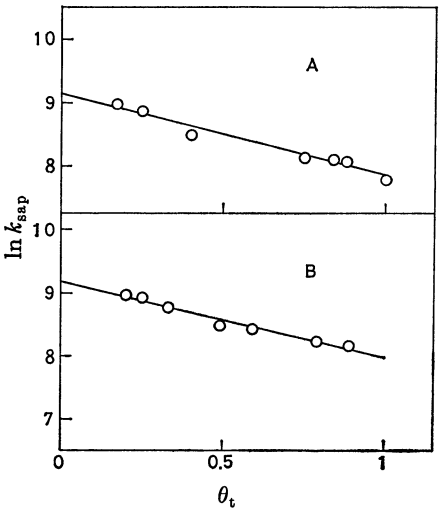

Fig. 9. Plots of ln k_{sap} against θ_t at (A) pH 6.9 and (B) pH 4.9.

Table 5. Electrochemical data of FMN adsorbed on a mercury electrode and in a bulk solution

pH	$k_{sap}(\theta_t\rightarrow0)$ / s^{-1}	a	K	E'_o *vs.* SCE / V	E'_{o1} *vs.* SCE / V	E'_{o2} *vs.* SCE / V	K(bulk)[a]	E'_o(bulk)[a] *vs.* SCE / V	E'_{o1}(bulk)[a] *vs.* SCE / V	E'_{o2}(bulk)[a] *vs.* SCE / V
6.9	9.5×10^3	1.3	1.1	−0.41	−0.41	−0.41	0.073	−0.45	−0.48	−0.42
4.9	9.7×10^3	1.2	0.72	−0.31	−0.31	−0.31	0.094	−0.34	−0.37	−0.31

a) Ref. 12.

References

1) W. R. Heineman and P. T. Kissinger, *Anal. Chem.*, **50**, 166R (1978).
2) K. D. Snell and A. G. Keenan, *Chem. Soc. Rev.*, **8**, 259 (1979).
3) T. Kakutani and M. Senda, *Bull. Chem. Soc. Jpn.*, **52**, 3236 (1979).
4) T. Kakutani and M. Senda, *Bull. Chem. Soc. Jpn.*, **53**, 1942 (1980).
5) T. Ikeda, K. Toriyama, and M. Senda, *Bull. Chem. Soc. Jpn.*, **52**, 1937 (1979).
6) T. Kakutani, K. Toriyama, T. Ikeda, and M. Senda, *Bull. Chem. Soc. Jpn.*, **53**, 947 (1980).
7) G. Dryhurst, "Electrochemistry of Biological Molecules", Academic Press, New York (1977).
8) M. Senda, M. Senda, and I. Tachi, *Rev. Polarogr. (Kyoto)*, **10**, 142 (1962).
9) Y. Takemori, *Rev. Polarogr. (Kyoto)*, **12**, 63 (1964).
10) A. M. Hartley and G. S. Wilson, *Anal. Chem.*, **38**, 681 (1966).
11) B. Breyer and T. Biegler, *Collect. Czech. Chem. Commun.*, **25**, 3348 (1960).
12) R. D. Draper and L. L. Ingraham, *Arch. Biochem. Biophys.*, **125**, 802 (1968).
13) J. Koryta, *Collect. Czech. Chem. Commun.*, **18**, 206 (1953).
14) R. A. Harie, "Molecules in Three Dimensions," Am. Soc. of Biol. Chem. Inc., Bethesda, Meryland, U.S.A.